

# Influence of End Groups on Phase Behavior and Properties of PEO in Aqueous Solutions

Elena E. Dormidontova\*

Department of Macromolecular Science and Engineering, Case Western Reserve University, Cleveland, Ohio 44106

Received October 25, 2003; Revised Manuscript Received June 24, 2004

**ABSTRACT:** The influence of the different terminal groups (hydroxyl, methyl) on the properties and phase behavior of PEO in aqueous solutions has been studied analytically. We have generalized our previous model to account for the competition for proton donors and acceptors among four types of hydrogen bonding (donors are mentioned first): water–PEO, water–water, PEO–water, and PEO–PEO. We found that for PEO terminated at both ends by methyl groups the influence of the end groups is minor, similar to infinitely long PEO. Termination of PEO by hydroxyl groups results in hydration enhancement in the poor hydration regions, i.e., at high polymer concentration (low water content) and at high temperature. The contribution of end groups to overall hydration is especially strong for short polymer chains and decreases with chain length as  $1/N$ , but it remains larger than 1% for chains with  $N \lesssim 250$  (for equal fraction of polymer and solvent,  $\Phi = 0.5$ ) or with  $N \lesssim 460$  (for  $\Phi = 0.9$ ). For a polymer volume fraction less than about 0.886, the contribution of end group to hydration increases with temperature and for polymer solutions of higher concentration it decreases with temperature (due to competition with PEO–PEO hydrogen bonding). We also discuss the possibility of physical cross-linking of PEO either via direct PEO–PEO hydrogen bonds or via a single water molecule acting as a cross-linking agent. We found that the degree of cross-linking considerably increases with chain length and also is strongly enhanced for hydroxyl-terminated short chains. Hydration via end groups also results in a chain length dependence of the second virial coefficient,  $A_2$ . For one- or two-end hydroxyl-terminated PEO, the second virial coefficient decreases with a chain length increase whereas for the methyl-terminated PEO  $A_2$  increases with an increase in chain length, tending to the same constant limit for infinitely long chains. The phase diagram calculated accounting for hydration via terminal hydroxyl groups features considerably improved agreement between theoretical predictions and experimental observations for short PEO chains: theoretical curves become more centered around experimental data and the chain lengths used for calculations are close to the molecular weight of experimental samples. Theoretical predictions become more consistent for the whole range of chain lengths studied. As a result the lower (LCST) and upper critical solution temperatures (UCST) for hydroxyl-terminated PEO agree very well with different experimental data. Comparing the critical points (UCST and LCST) for polymer chains terminated by different end groups we found that while all curves merge in the long chain limit ( $N > 300$  for LCST and  $N > 500$  for UCST), for shorter chain lengths curves deviate from each other considerably, reaching double critical points (where the UCST merges with the LCST) at different  $N$ . Termination of PEO by one hydroxyl group improves the solubility of PEO chains to an extent that it is equivalent to decreasing of chain length by 10 monomer units and adding a second hydroxyl group doubles the effect.

## Introduction

Aqueous solutions of poly(ethylene oxide) have attracted considerable attention during recent decades.<sup>1–11</sup> In contrast to normal polymer behavior in which the solubility increases with temperature (unless there is a compressibility-driven phase separation<sup>12</sup>), the solubility of PEO decreases (as does the second virial coefficient<sup>5,6</sup>) and phase separation occurs above a critical temperature that depends on the molecular weight.<sup>1–4</sup> The reason for such unusual behavior is hydrogen bonding between PEO and water, which competes with water–water hydrogen bonding, as we discussed in our previous paper.<sup>7</sup> Besides the purely academic interest in the unusual behavior of this polymer, PEO has also attracted attention because of its practical importance.<sup>13,14</sup> PEO is biocompatible and inhibits protein adsorption, a property that finds extensive applications in surface modification and drug delivery.<sup>13,14</sup> Thus, it is evident that an understanding of the behavior of poly(ethylene oxide) in aqueous solutions is very desirable.

As is well understood both experimentally and theoretically, hydrogen bonding (hb) in aqueous solutions

of PEO is of key importance for understanding the behavior of PEO in water.<sup>3,4,7–11</sup> Besides the above-mentioned PEO–water and water–water hydrogen bonding where hydrogens of water act as proton donors, there are other types of hydrogen bonding that depend on the PEO end groups. There are three typical end groups for PEO (Figure 1). Most common is PEO terminated by hydroxyl groups at both ends. Additionally there is PEO terminated by a hydroxyl group at one end and by methyl group at another or methyl groups at both ends. For hydroxyl-terminated PEO, there is an additional source of proton donors which provide two additional types of hydrogen bonding: PEO–water and PEO–PEO. These two types of hydrogen bonding compete with each other and with water–PEO and water–water hydrogen bonding. Having an additional source for hydrogen bonding between PEO and water via terminal groups may improve the overall hydration of PEO and influence solubility and other properties of PEO.

Experimentally, it has been observed that the replacement of hydroxyl end groups by more hydrophobic groups (less capable of formation of hydrogen bonds with water) considerably decreases the lower critical solution temperature (LCST) of aqueous solutions of PEO 500.<sup>15</sup>

\* E-mail: eed@po.cwru.edu.

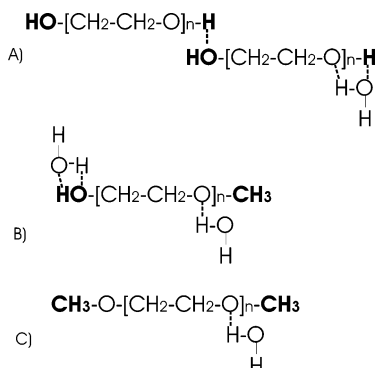


**Figure 1.** Schematic presentation of poly(ethylene oxide) (PEO) terminated by different end groups (hydroxyl groups at both ends (A), hydroxyl group at one end and methyl group at the other (B) and methyl groups at both ends (C)) with indication of hydrogen bonding taking place between PEO (for hydroxyl groups) and between water and PEO in each of the cases.

Also, the recent study of the partitioning of PEO of different molecular weights between water and organic phases ( $\text{CH}_2\text{Cl}_2$  or  $\text{CHCl}_3$ ) has shown that replacement of hydroxyl end groups by methyl groups has a dramatic effect on the partition coefficients.<sup>16</sup> The increased partition of methyl-terminated PEO into an organic phase is much larger than any estimated increase due to the addition of two methyl groups. Evidently the difference must be in the participation of the hydroxyl and methyl groups in hydrogen bonding with water. Studying the change in the partition coefficient with the molecular weight of PEO, Loh and coauthors came to the conclusion that the end-effect contribution becomes insignificant for polymers exceeding ca. 3000 g/mol.<sup>16</sup> In general the boundary between poly(ethylene glycol), where end-effects can be noticeable, and poly(ethylene oxide), where the influence of end groups is minor, is placed by chemical companies between 3350 and 10000 g/mol.<sup>16</sup> Another recent study has been concerned with the influence of the end groups on the phase boundaries in PS/PEO homopolymer blends and PS-PEO diblock copolymer melts.<sup>17</sup> It has been found that the change from a hydroxyl to a methoxy terminal group on PEO in polymer blends resulted in the decrease in the upper critical solution temperature (UCST) by up to 90°, whereas for PS-PEO diblock copolymers the order-disorder transition point shifted lower by about 45°. As we can see, several experimental studies<sup>15–17</sup> confirm that the effect of end groups of PEO can be quite considerable, especially when it concerns the phase behavior of a polymer which reflects the delicate balance of translational entropy, volume interactions, and hydrogen bonding.

Despite the experimental interest in the influence of end groups on the behavior of PEO,<sup>15–17</sup> theoretical predictions on this subject are missing so far. The present paper has the aim to change this situation and to study analytically what features of the behavior of PEO are seriously influenced by end groups and when this influence is important. To this end we will modify our previous model<sup>7</sup> to account for the two other types of hydrogen bonding that arise from the proton donation from PEO hydroxyl end groups and will consider the competition between the four types of hydrogen bonds present in hydroxyl-terminated PEO. In particular we will analyze the influence of end groups on PEO hydration and will study how different end groups influence the second virial coefficient and phase behav-

ior of PEO. The comparison with experimental data and results of our previous model neglecting end effects<sup>7</sup> will be made.

Another issue which has been discussed experimentally over the years is whether there is cluster formation in aqueous solutions of PEO.<sup>5,18–21</sup> Molecular weight, temperature and concentration dependence of the cluster formation (when observed)<sup>5,18,21</sup> implies that this may be the result of hydrogen bonds. However, water can also be considered as a network of hydrogen bonds, but in its physical behavior it does not act as a typical gel. Therefore, not all hydrogen bonding can lead to cluster (gel) formation. Below we will consider two types of the most direct cross-linking of PEO: via direct PEO-PEO hydrogen bonding and via a single water-molecule acting as a cross-linking agent. In this approximation, we will estimate the boundary for the possible gel formation and analyze the influence of end groups on this boundary.

This paper is arranged in the following manner. In the next section we will describe the details of our model, which we will use to analyze the behavior of end groups of PEO in aqueous solutions. In the section "Results and Discussion" we will consider the results of our model as concerns the average degree of association for different types of hydrogen bonding, its concentration and temperature behavior. We will also study the contribution of the end groups to overall hydration as a function of chain length, temperature, and concentration and analyze the possibility of a gel formation (by means of hydrogen bonds) for PEO chains with different end groups. Finally we will also discuss the influence of additional hydration via end groups on the second virial coefficient and phase behavior of PEO in aqueous solutions. Predictions of our model will be compared with experimental data. The main results discussed in this paper will be summarized in the "Conclusions" section.

## Model

We will consider aqueous solutions of PEO chains terminated by different end groups: hydroxyl groups at both ends, a methyl group at one end with a hydroxyl group at the other, and methyl groups at both ends (Figure 1). The number of repeat units in the PEO chains is  $N$  with the monomer unit volume  $v_p$ . End groups also occupy some volume, which differs depending on the end groups. Since in what follows we will mainly use the ratio between the volumes occupied by end groups and repeat unit,  $v_e$ , we will use for this value the ratio of corresponding molar volumes; i.e.,  $v_e = 18/44$  for hydroxyl-terminated ends,  $v_e = 32/44$  for one hydroxyl and one methyl end, and  $v_e = 46/44$  for both methyl ends. As in our previous model,<sup>7</sup> the volume of a water molecule,  $v$ , will be considered as a reference volume, i.e., the volume of a cell in Flory-Huggins theory. The specificity of the PEO and water molecules in hydrogen bond formation will be captured via the characteristic energetic and entropic change upon hb formation which we will estimate based on experimentally reported data. Depending on the chemical nature of the end groups, there might be up to four different types of hydrogen bonds. For both ends, methyl-terminated PEO there are only two types of hydrogen bonding, water-water and water-PEO hydrogen bonds, for which the hydrogen of water acts as the proton donor. Competition of these hydrogen bonds has been considered in our previous model for long PEO chains

(neglecting end effects),<sup>7</sup> so that the behavior of methyl-terminated PEO is expected to be similar to that predicted by this model.<sup>7</sup> For one or two-end hydroxyl-terminated PEO there are two more types of hydrogen bonding: PEO–water and PEO–PEO for both of which the hydrogen of the hydroxyl group acts as a proton donor. In such a case there is an interplay between the four types of hydrogen bonds: besides the competition for proton donors, mentioned above, acceptors of PEO and water also have to be shared between different proton donors.

To obtain the free energy of the hydrogen bonded solution, we will modify our previous model<sup>7</sup> (which was based on the approach of Semenov and Rubinstein for solutions of associated polymers.<sup>22</sup>) The free energy (density) of the system can be presented in the following form:

$$F = F_{\text{ref}} + F_{\text{int}} + F_{\text{assoc}} \quad (1)$$

The reduced free energy (per unit cell) of the reference state,<sup>23</sup> a solution of noninteracting polymers,  $F_{\text{ref}}$ , has purely entropic character and is defined by

$$\frac{F_{\text{ref}}}{kT} = \frac{\Phi v}{(N + v_e)v_p} \ln \left( \frac{\Phi v}{(N + v_e)v_p e} \right) + (1 - \Phi) \ln((1 - \Phi)/e) \quad (2)$$

where  $\Phi$  is the volume fraction of polymer.

$F_{\text{int}}$  describes the (volume) interactions between polymer and solvent monomers, apart from the hydrogen bonding:

$$\frac{F_{\text{int}}}{kT} = \Phi \chi (1 - \Phi) \quad (3)$$

where  $\chi$  is the interaction parameter in the Flory–Huggins model for PEO–water volume interactions in the absence of hydrogen bonding. We note that in eq 3 we considered an “averaged”  $\chi$ -parameter for the polymer–solvent interaction without specifying the contribution of end groups. It would be desirable to account for volume interactions between end groups and between end groups and solvent. However, having no experimentally tested temperature dependencies of such parameters, we had to assume that the end group contribution to the volume interactions (apart from hydrogen bonding) is similar to that of the repeat units. In any case, it is known that the  $\text{CH}_3$  group is more hydrophobic and the OH group more hydrophilic compared to the repeat unit of PEO, which follows the trend expected based on hydrogen bonding only. Therefore, if there is any effect of volume interactions of the end groups in addition to the hydrogen bonding effects considered below, it will be only a magnifying and not a counteracting factor.

$F_{\text{ref}} + F_{\text{int}}$  represents the free energy of a nonassociated polymer solution (having the traditional random-mixing Flory–Huggins form). We note that the applied random-mixing approach does not account for detailed microscopic mechanisms of polymer solvation, as is typical of the mean-field approximation. In particular the results of the approach in the case of very dilute polymer solutions should be considered with care. For a nonassociated polymer solution one can expect an increase of polymer solubility with temperature (unless compressibility effects interfere). Hydrogen bonding

between polymer and solvent (and between polymers or solvent molecules) alters the situation by changing both the translational entropy (degree of mixing) and volume interactions (resulting, e.g., in additional contributions to the  $\chi$ -parameter, as discussed in our previous paper<sup>7</sup> and below).

$F_{\text{assoc}}$  is the part of the free energy due to PEO–water and water–water hydrogen bonding, which can be written in the following form:<sup>7,22,24</sup>

$$\frac{F_{\text{assoc}}}{kT} = - \frac{v}{V} \ln Z_{\text{assoc}} \quad (4)$$

where  $Z_{\text{assoc}}$  is the following partition function

$$Z_{\text{assoc}} = P_{\text{comb}} \prod_{i=\text{ww,wp,pw}} \left[ W_i \exp \left( \frac{\Delta E_i}{kT} n_i \right) \right] \quad (5)$$

where  $i = \text{ww, wp, pw, and pp}$  denote the types of hydrogen bonds (proton donors mentioned first): water–water (ww), water–PEO (wp), PEO–water (pw) and PEO–PEO (pp).  $\Delta E_i$  is the energetic gain for formation a hydrogen bond of type  $i$ .  $W_i$  is the probability that the donor and acceptor groups can be found in the vicinity of each other and with the correct orientation for formation of a hydrogen bond. We note that  $W_i$  should be considered only in the conjunction with the other terms of the partition function (eq 5). Thus,  $W_i$  depends on the volume of the system and  $P_{\text{comb}}$  depends on the absolute number of donor (acceptors), whereas  $Z_{\text{assoc}}$  (and the resulting free energy) as a whole depends only on the concentration of the donor (acceptor) groups. At the moment we will describe  $W_i$  in a somewhat generalized way,<sup>7,22</sup> whereas later we will assign its different parts to particular physical effects.

$$W_i = \left( \frac{v_{\text{hb}}^i}{V} \right)^{n_i} \quad (6)$$

where  $V$  is the volume of the system and  $v_{\text{hb}}^i$  is the volume per hydrogen bond of type  $i$ . We note that in the present model any atomistic details of the chain structure are omitted. Therefore, our model is not expected to account correctly for the possibility of PEO ring formation by means of PEO–PEO hydrogen bonding in a very dilute solution or for any cooperativity in hydrogen bond formation enforced by chain conformations, e.g., in the crystallization region. The former may not be of much effect anyway as in the dilute region most of the hydrogens of hydroxyl groups are hydrogen bonded with water and the latter has a little impact on solubility and phase behavior of PEO, which is of our primary concern here.

$P_{\text{comb}}$  is the combinatorial factor describing the number of ways to form all  $n_i$  hydrogen bonds. Each molecule of water carries two hydrogens which can participate in the formation of hydrogen bonds either with PEO or with other water molecules, hence the total number of proton donors of water is  $2N_{\text{w}}$ , where  $N_{\text{w}}$  is the number of water molecules. Similarly each oxygen of water can accept two hydrogen bonds, and the total number of proton acceptors on water is also  $2N_{\text{w}}$ . Each repeat oxygen of PEO can participate in formation of two hydrogen bonds, as can the oxygens of the end groups. In general, oxygens of hydroxyl groups tend to form stronger hydrogen bonds with water (most likely due to better accessibility and a smaller entropic penalty for



hydrogen bonding), although to simplify our model we will omit the difference between the oxygens of the hydroxyl groups and repeat units of PEO. We believe that by making this assumption we do not inflict any noticeable error in our predictions because, as we will see below, the main impact of the end groups occurs in poor hydration conditions when the occupancy of oxygens of PEO is not so high. Therefore, the somewhat stronger hydrogen bonds with a hydroxyl group oxygen would only slightly increase the overall hydration. Thus, the total number of proton acceptors on PEO chain is  $2\mathcal{N}_p(N + m_o)$ , where  $\mathcal{N}_p$  is the number of PEO chains and  $m_o$  is the number of oxygens on end groups ( $m_o = 1$  for all end groups considered). The proton donors of PEO are exclusively on the hydroxyl groups, so that the total number of PEO proton donors is  $\mathcal{N}_p m_h$ .  $m_h$  is the number of proton-donating hydrogens on the end groups ( $m_h = 1$  for a hydroxyl group and  $m_h = 0$  for a methyl group). We note that accounting for the total number of proton donors and acceptors we consider all of them to be potentially accessible for hydrogen bonding. Knowing the total numbers of donors and acceptors in the polymer system, we can calculate the combinatorial factor in a way similar to that described in refs 7 and 22:

$$P_{\text{comb}} = \frac{(2\mathcal{N}_p(N + m_o))!}{(2\mathcal{N}_p(N + m_o) - n_{\text{wp}} - n_{\text{pp}})!n_{\text{wp}}!} \times \frac{(\mathcal{N}_p m_h)!}{(2\mathcal{N}_w)!} \times \frac{(2\mathcal{N}_w)!}{(2\mathcal{N}_p m_h - n_{\text{pw}} - n_{\text{pp}})!n_{\text{pp}}!} \times \frac{(2\mathcal{N}_w)!}{(2\mathcal{N}_w - n_{\text{ww}} - n_{\text{pw}})!n_{\text{ww}}!} \quad (7)$$

Using eqs 1–7, the total free energy (per unit cell) of the polymer system can be presented in the form

$$\begin{aligned} \frac{F}{kT} = & \frac{\Phi v}{(N + v_e)v_p} \ln\left(\frac{\Phi v}{(N + v_e)v_p}\right) + (1 - \Phi) \ln((1 - \Phi)/e) + \\ & \chi\Phi(1 - \Phi) + 2\Phi \frac{(N + m_o)v}{(N + v_e)v_p} \times \\ & \left[ x \ln x + (1 - x) \ln\left(1 - x - s \frac{m_h}{2(N + m_o)}\right) - x \frac{\Delta F_{\text{wp}}}{kT} \right. \\ & \left. - x \ln(2(1 - \Phi)/e) - x \ln\left(1 - y - x \frac{\Phi(N + m_o)v}{(1 - \Phi)(N + v_e)v_p}\right) \right] + \\ & \frac{\Phi m_h v}{(N + v_e)v_p} \times \\ & \left[ u \ln u + (1 - u - s) \ln(1 - u - s) - u \frac{\Delta F_{\text{pw}}}{kT} - u \ln(2(1 - \Phi)/e) \right. \\ & \left. - u \ln\left(1 - y - u \frac{\Phi m_h v}{2(1 - \Phi)(N + v_e)v_p}\right) \right] + \\ & \frac{\Phi m_h v}{(N + v_e)v_p} \left[ s \ln s - s \ln\left(1 - x - s \frac{m_h}{2(N + m_o)}\right) - s \frac{\Delta F_{\text{pp}}}{kT} - \right. \\ & \left. s \ln\left(\frac{2\Phi(N + m_o)v}{(N + v_e)v_p e}\right) \right] + 2(1 - \Phi) \left[ y \ln y - y \ln(2(1 - \Phi)/e) - \right. \\ & \left. y \frac{\Delta F_{\text{ww}}}{kT} + (1 - y) \ln\left(1 - y - x \frac{\Phi(N + m_o)v}{(1 - \Phi)(N + v_e)v_p}\right) \right] + \\ & 2(1 - \Phi)(1 - y) \ln\left(1 - y - u \frac{\Phi m_h v}{2(1 - \Phi)(N + v_e)v_p}\right) \quad (8) \end{aligned}$$

where we introduced the new variables, the average fraction of hydrogen bonds of each kind:

$$x \equiv \frac{n_{\text{wp}}}{2\mathcal{N}_p(N + m_o)}; \quad y \equiv \frac{n_{\text{ww}}}{2\mathcal{N}_w}; \quad u \equiv \frac{n_{\text{pw}}}{\mathcal{N}_p m_h}; \quad s \equiv \frac{n_{\text{pp}}}{\mathcal{N}_p m_h} \quad (9)$$

In eq 8 we also used the relation between the number of PEO or water molecules and their volume fractions:  $\mathcal{N}_p(N + v_e)v_p/V \equiv \Phi$ ,  $\mathcal{N}_w v/V \equiv (1 - \Phi)$ . In addition we combined the contributions for the energetic gain and entropic loss for hydrogen bond formation in one term:

$$\frac{\Delta F_i}{kT} \equiv \frac{\Delta E_i}{kT} - \Delta S_i \quad (10)$$

where the entropic loss is defined by

$$\Delta S_i \equiv - \ln \frac{v_{\text{hb}}^i}{v} \equiv - \ln \frac{1 - \cos \Delta_i}{2} \quad (11)$$

As we have mentioned in our previous paper,<sup>7</sup> the entropic loss for formation of a hydrogen bond is connected with the loss of orientational entropy for the donor and acceptor groups which have to keep the correct orientation inside the characteristic space angle  $\Delta$  for the hydrogen bond to remain stable. Therefore, the entropic loss for hydrogen bond formation can be characterized via the critical angle,  $\Delta_i$ . The values of the characteristic angle (or entropy of association) for hb formation can be estimated from experimental data.

We note that as expected in the limit of  $u \rightarrow 0$ ,  $s \rightarrow 0$  and  $m_h = 0$ ,  $m_o = 0$ , eq 8 recovers the expression for the free energy obtained in our previous paper for long PEO chains (neglecting end effects).<sup>7</sup>

Minimization of the free energy (eq 8) with respect to the average fraction of water–PEO,  $x$ , water–water,  $y$ , PEO–water,  $u$ , and PEO–PEO hydrogen bonds,  $s$ , leads to the following equations, respectively

$$x = \exp\left(\frac{\Delta F_{\text{wp}}}{kT}\right) \left(1 - x - s \frac{m_h}{2(N + m_o)}\right) \times \left(1 - y - x \frac{\Phi(N + m_o)v}{(1 - \Phi)(N + v_e)v_p}\right) 2(1 - \Phi) \quad (12)$$

$$y = \exp\left(\frac{\Delta F_{\text{ww}}}{kT}\right) \left(1 - y - x \frac{\Phi(N + m_o)v}{(1 - \Phi)(N + v_e)v_p}\right) \times \left(1 - y - u \frac{\Phi m_h v}{2(1 - \Phi)(N + v_e)v_p}\right) 2(1 - \Phi) \quad (13)$$

$$s = \exp\left(\frac{\Delta F_{\text{pp}}}{kT}\right) (1 - u - s) \times \left(1 - x - s \frac{m_h}{2(N + m_o)}\right) \frac{2\Phi(N + m_o)v}{(N + v_e)v_p} \quad (14)$$

$$u = \exp\left(\frac{\Delta F_{\text{pw}}}{kT}\right) (1 - u - s) \times \left(1 - y - u \frac{\Phi m_h v}{2(1 - \Phi)(N + v_e)v_p}\right) 2(1 - \Phi) \quad (15)$$

The set of these four equations defines the equilibrium degree of association for the four types of hydrogen

bonds. For the numerical solution of the set of equations it is useful to express two of the variables, e.g.,  $s$  and  $u$  via the other two as

$$\frac{1}{u} = 1 + \frac{1}{y} \exp\left(\frac{\Delta F_{ww} - \Delta F_{pw}}{kT}\right) \times \left(1 - y - x \frac{\Phi(N + m_0)v}{(1 - \Phi)(N + v_e)v_p} \times \left(1 - \exp\left(\frac{\Delta F_{pp} - \Delta F_{wp}}{kT}\right)\right)\right) \quad (16)$$

$$s = x \frac{u}{y} \exp\left[\frac{\Delta F_{pp} + \Delta F_{ww} - \Delta F_{wp} - \Delta F_{pw}}{kT}\right] \times \frac{\Phi(N + m_0)v}{(1 - \Phi)(N + v_e)v_p} \quad (17)$$

Equations 12–17 clearly show that there is a competition for proton donors and acceptors among the four types of hydrogen bonds. The results of this competition will be discussed in the next section.

## Results and Discussion

To calculate the average degree of association for the four types of hydrogen bonds one has to solve the above set of equations numerically. For the energies and entropies of water–PEO and water–water hydrogen bonding we will use the same values as in our previous paper,<sup>7</sup> i.e.,  $\Delta E_{wp}/k = 2000$  K,  $\Delta E_{ww}/k = 1800$  K and  $\Delta_{wp} = \pi/8.35$ ,  $\Delta_{ww} = \pi/4.75$ . As we mentioned in our previous paper these values (except  $\Delta_{wp}$  for which we used the value providing the best match with experimental data for the phase behavior) are based on experimental observations.<sup>25,26</sup> It is known from experimental studies that the enthalpy of PEO–PEO hydrogen bonding is about 14.87 kJ/mol,<sup>27</sup> that corresponds to  $\Delta E_{pp}/k = 1800$  K, which is the same as for water–water hydrogen bonding. The entropic loss for PEO–PEO hydrogen bond formation is expected to exceed that for water–PEO hydrogen bonding due to the architectures of the associating groups, so we will use  $\Delta_{pp} = \pi/10$ . We note that the choice of  $\Delta_{pp}$  does not have any noticeable impact on the principal results discussed below, so the only quantitative values which can be slightly altered are the sol–gel transition boundary and the end group hydration in the high polymer concentration region. Finally, PEO–water hydrogen bonding via terminal hydroxyl groups is known to be somewhat stronger than for water–PEO and we will use  $\Delta E_{pw}/k = 2200$  K, which corresponds to the upper limit of the experimentally estimated average enthalpy of hydrogen bonding between PEO and water.<sup>25</sup> The entropic loss for PEO–water hydrogen bonding is expected to be similar to water–water hydrogen bonding<sup>26</sup> due to the architecture of the reacting hydroxyl groups, so we will use  $\Delta_{pw} = \pi/5$ . To compare the results of the present model with the previous results obtained for long chains (neglecting end effects),<sup>7</sup> we will assume as before that  $v_p = 3v$ .

**The Average Degree of Association.** The concentration dependence of the average degree of water–PEO ( $x$ ), water–water ( $y$ ), PEO–water ( $u$ ), and PEO–PEO ( $s$ ) associations for hydroxyl-terminated PEO are presented in Figure 2 for  $N = 5$  and  $T = 20$  °C. In the low concentration range the average fraction of water molecules associated with another water molecule slightly

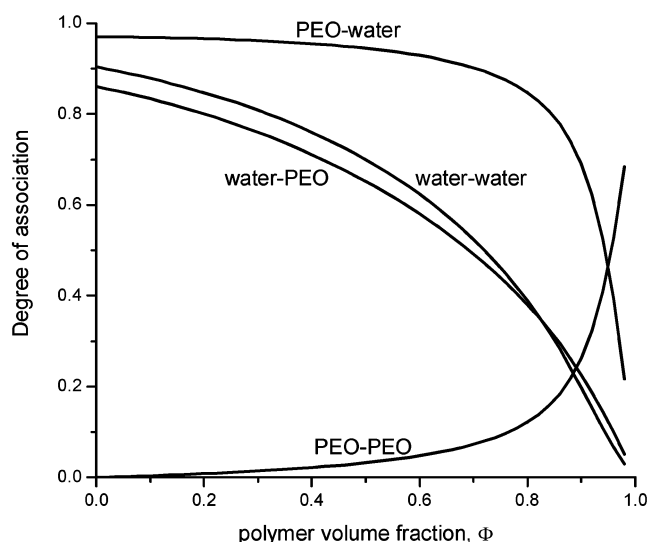


**Figure 2.** Concentration dependence of the average degree of association for PEO–water; water–water, water–PEO and PEO–PEO for hydroxyl-terminated PEO. The curves are obtained by solving eqs 12–15 for  $T = 20$  °C,  $N = 5$ ,  $\Delta E_{wp}/k = 2000$  K,  $\Delta E_{ww}/k = 1800$  K,  $\Delta E_{pp}/k = 1800$  K,  $\Delta E_{pw}/k = 2200$  K,  $\Delta_{wp} = \pi/8.35$ ,  $\Delta_{ww} = \pi/4.75$ ,  $\Delta_{pp} = \pi/10$ , and  $\Delta_{pw} = \pi/5$ .

exceeds that associated with PEO. Both degrees of association decrease with increasing concentration. This behavior is similar to the predictions of our previous model obtained for long PEO chains (neglecting end effects),<sup>7</sup> the absolute values for  $x$  and  $y$  in zero concentration limit coincide with that obtained in our previous model. However with an increase in polymer concentration the water–water degree of association decreases quicker than water–PEO and exhibits a small region of negative curvature at high polymer concentration. This was not the case for long PEO chains (neglecting end effects)<sup>7</sup> where both water–water and water–PEO degrees of association decrease at similar rates with increasing concentrations, so that the water–water degree of association always exceeded that for water–PEO. The reason for this difference is the competition for water acceptors between the water–water and PEO–water associations. PEO–water association via proton donation from hydroxyl groups is the most favorable interaction among the four. As a result, all hydrogens of hydroxyl groups remain totally occupied (even at the expense of the water–water association) except at high polymer concentrations ( $\Phi \lesssim 0.88$ ). At high polymer concentration there are not enough free water acceptors for proton donation from PEO hydroxyl groups and PEO–PEO association becomes favorable. A similar concentration dependence is observed for longer polymer chains, except that the decline of the PEO–water association and corresponding enhancement of PEO–PEO association occurs at higher polymer concentrations. Also, for longer polymer chains the water–water degree of association exceeds that for water–PEO hydrogen bonding over the whole concentration range, as we mentioned above.

The degrees of association of different types also change with temperature. An example of the temperature dependence for concentrated solutions of PEO is shown in Figure 3 for  $N = 5$  and  $\Phi = 0.9$ . In general, the gain in enthalpy of hydrogen bonding compared to  $kT$  decreases with the temperature increase and the extent of hydrogen bonding decreases as well. This observation is correct for all types of associations at high

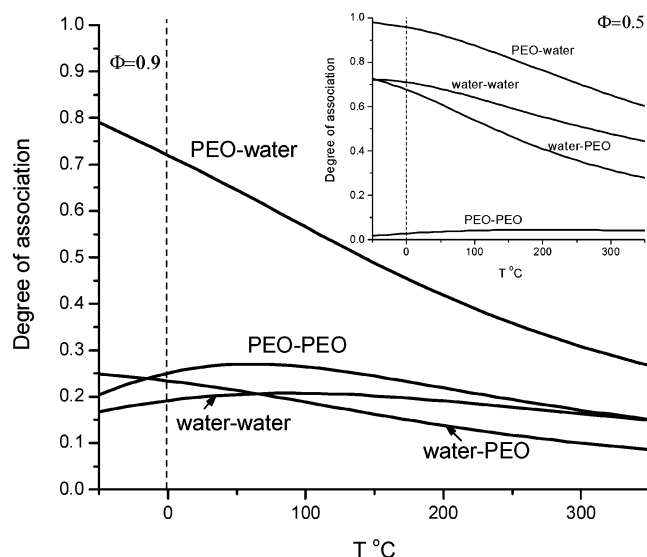


**Figure 3.** Temperature dependence of the average degree of association for PEO–water, PEO–PEO, water–water, and water–PEO for hydroxyl-terminated PEO. The curves are obtained by solving eqs 12–15 for  $N = 5$ ,  $\Delta E_{wp}/k = 2000$  K,  $\Delta E_{ww}/k = 1800$  K,  $\Delta E_{pp}/k = 1800$  K,  $\Delta E_{pw}/k = 2200$  K,  $\Delta_{wp} = \pi/8.35$ ,  $\Delta_{ww} = \pi/4.75$ ,  $\Delta_{pp} = \pi/10$ ,  $\Delta_{pw} = \pi/5$ ,  $\Phi = 0.9$ , and  $\Phi = 0.5$  (inset).

temperature (Figure 3). At lower temperatures the average degree of interspecies (polymer–solvent) types of hydrogen bonding (i.e., PEO–water and water–PEO) decreases as well, whereas that of intraspecies associations (polymer–polymer, or solvent–solvent) actually increases in some temperature ranges, achieving a maximum at about  $T = 60$  °C for PEO–PEO association and at  $T = 90$  °C for water–water association shown in Figure 3. Evidently the distribution of proton donors from water–PEO to water–water and from PEO–water to PEO–PEO hydrogen bonding occurs. At higher temperatures, the redistribution of proton donors (acceptors) continues as water–water and PEO–PEO hydrogen bonding decreases at a slower pace compared to polymer–solvent hydrogen bonding. This tendency, which holds at lower polymer concentration as well, explains the physical origin of the experimentally observed temperature-induced phase separation in aqueous solutions of PEO.<sup>1–6</sup> At a lower polymer volume fraction,  $\Phi = 0.5$ , shown in the insert, the PEO–water and water–PEO degree of hydrogen bonding decreases at a similar rate exceeding that for water–water and PEO–PEO. The position of the maxima for the water–water degree of association shifts to much lower temperature ( $T = -55$  °C), whereas the maximum for PEO–PEO degree of association shifts to considerably higher temperature ( $T = 200$  °C). The absolute value for the PEO–PEO association remains at a very low level even at its maximum whereas water–water association is stronger at the equal fraction of polymer and water compared to  $\Phi = 0.9$ . These observations are consistent with the concentration dependence discussed above (Figure 2).

**Hydration.** Hydration of a PEO is an important characteristic defining its solubility (phase behavior) and influencing some other important properties as, e.g., capability of protein adsorption. Experimentally hydration of PEO is evaluated by its hydration number, which is a complex characteristic of hydrogen bonded water surrounding PEO. For instance, the hydration number

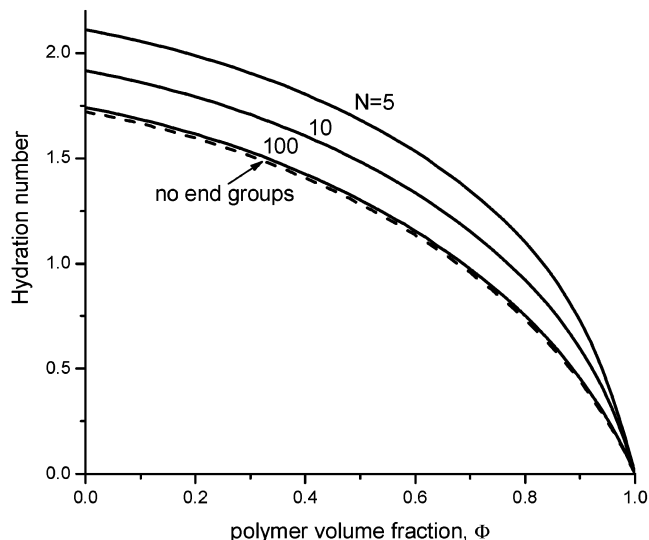


**Figure 4.** Concentration dependence of the hydration number (number of water molecules hydrogen bonded with PEO) per monomer unit of hydroxyl-terminated polymer. The curves are obtained using eq 18 for  $T = 20$  °C,  $N = 5, 10, 100$ ,  $\Delta E_{wp}/k = 2000$  K,  $\Delta E_{ww}/k = 1800$  K,  $\Delta E_{pp}/k = 1800$  K,  $\Delta E_{pw}/k = 2200$  K,  $\Delta_{wp} = \pi/8.35$ ,  $\Delta_{ww} = \pi/4.75$ ,  $\Delta_{pp} = \pi/10$ , and  $\Delta_{pw} = \pi/5$ .

can be considered as the number of water molecules which can be packed on the surface of a PEO monomer.<sup>28</sup> Depending on the experimental technique applied and the range of concentrations studied, the hydration number can vary from one to six water molecules per PEO unit at fixed temperature.<sup>28–30</sup> Since we do not consider any atomistic details of PEO or water structure, we will define the hydration number as the number of water molecules directly hydrogen bonded to PEO per monomer unit of PEO, i.e.

$$N_{\text{hydr}} = \frac{2(N + m_0)}{N}x + \frac{m_h}{N}u \quad (18)$$

The concentration dependence of the hydration number for both end hydroxyl-terminated PEO is shown in Figure 4 for different chain lengths at  $T = 20$  °C. At low polymer concentration the hydration number is maximal due to the excess of solvent. With concentration increase the hydration number decreases for all considered chain lengths and reaches nearly zero level at high polymer concentration. In general, the shorter the PEO chain length the higher the hydration (per repeat unit) in the whole concentration range. For shorter chains the relative contribution of end group hydration is obviously larger compared to longer chains and so the hydration number. For long polymer chains the contribution of end groups becomes insignificant and they behave similarly to what is expected in the model neglecting end effects.<sup>7</sup>

Taking into account that influence of end groups on overall chain hydration decreases with chain length, the following question arises: What is the critical chain length when contribution of end groups is still noticeable? To answer this question, we will consider the relative contribution of the hydration of end groups to the overall chain hydration. We will define the relative hydration as the ratio of the number of water molecules directly hydrogen bonded to the end groups to the number of water molecules directly hydrogen bonded



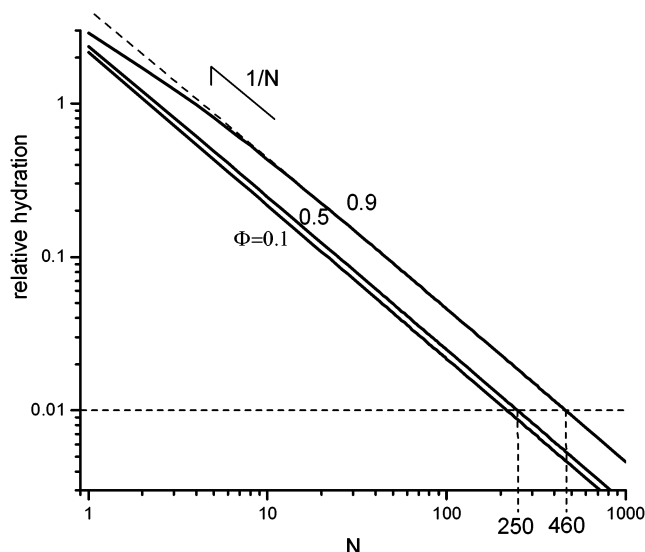


**Figure 5.** Relative hydration (ratio of the number of water molecules hydrogen bonded to end groups to that hydrogen bonded to the repeat units of PEO) for hydroxyl-terminated PEO as a function of chain length for different polymer volume fractions and  $T = 20\text{ }^{\circ}\text{C}$ ,  $\Delta E_{wp}/k = 2000\text{ K}$ ,  $\Delta E_{ww}/k = 1800\text{ K}$ ,  $\Delta E_{pp}/k = 1800\text{ K}$ ,  $\Delta E_{pw}/k = 2200\text{ K}$ ,  $\Delta_{wp} = \pi/8.35$ ,  $\Delta_{ww} = \pi/4.75$ ,  $\Delta_{pp} = \pi/10$ , and  $\Delta_{pw} = \pi/5$ . Critical chain lengths corresponding to the points where the relative hydration reaches 1% are indicated.

to the main chain, i.e.

$$\frac{\text{hydration via end groups}}{\text{hydration of the main chain}} = \frac{m_h u + 2m_o x}{2Nx} \quad (19)$$

The chain length dependence for the relative hydration for hydroxyl-terminated PEO is shown in Figure 5 in double logarithmic scale for  $T = 20\text{ }^{\circ}\text{C}$  and different polymer content. As is expected from eq 19, the relative hydration varies according to a  $1/N$  law regardless the polymer content, especially at high  $N$ . For low polymer concentration the relative hydration decreases with an increase in PEO chain length very similar to the  $2/N$ . At higher concentration the absolute value of the relative hydration slightly increases, as in this area both hydrogens and oxygen of the end groups fully participate to hydration. We note that for  $\Phi = 0.9$  the chain length dependence deviate from  $1/N$  for small  $N$ . The reason for this is partial involvement of hydrogens from hydroxyl groups in PEO–PEO hydrogen bond formation. The shorter the PEO the larger participation of the hydrogens of hydroxyl groups in PEO–PEO hydrogen bonding (Figure 2) and the larger is the deviation from a  $1/N$  law. In general, the contribution of the hydration via end groups remains noticeable up to relatively long PEO chains. For short chains ( $N \lesssim 10$ ) the contribution of the hydration via end groups is comparable with overall hydration. For long chains, the contribution of end groups to overall hydration is smaller, however its absolute level depends on polymer content. Thus, for equal fraction of polymer and solvent the contribution of end group hydration reaches 1% for PEO chain with 250 monomer units, whereas for  $\Phi = 0.9$  the 1% level is reached for chains nearly twice as long ( $N = 460$ ). For high polymer concentrations the contribution of the hydration via end groups increases although the absolute value of hydration decreases (Figure 4). This implies that water favors association with hydroxyl end groups and remains hydrogen bonded to the end groups

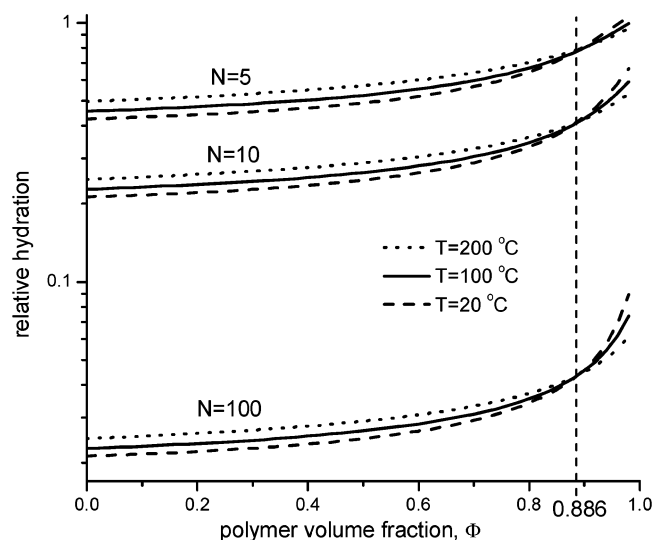


**Figure 6.** Concentration dependence of the relative hydration (ratio of the number of water molecules hydrogen bonded to end groups to that hydrogen bonded to the repeat units of PEO) for hydroxyl-terminated PEO calculated at different temperatures for  $N = 5$ ,  $N = 10$  and  $N = 100$ . The curves are obtained for  $\Delta E_{wp}/k = 2000\text{ K}$ ,  $\Delta E_{ww}/k = 1800\text{ K}$ ,  $\Delta E_{pp}/k = 1800\text{ K}$ ,  $\Delta E_{pw}/k = 2200\text{ K}$ ,  $\Delta_{wp} = \pi/8.35$ ,  $\Delta_{ww} = \pi/4.75$ ,  $\Delta_{pp} = \pi/10$ , and  $\Delta_{pw} = \pi/5$ .

even when overall hydration becomes poor. Therefore, the contribution of end groups to overall hydration becomes especially important in the poor hydration conditions (e.g., low solvent concentration) (Figure 5).

Since the degree of hydrogen bonding is generally decreasing with temperature increase, one would expect that the relative hydration may also vary with temperature. Indeed, Figure 6 confirms these expectations. In a wide concentration range, the relative hydration increases with temperature increase, supporting the conclusion that water remains attached to the hydroxyl groups even when it gets detached from the repeat units. At the same time, at high polymer concentration, we observe the opposite behavior as the relative hydration decreases with temperature increase. The reason for this is the interference of PEO–PEO hydrogen bonding which competes with PEO–water association. The boundary between the low and high concentration regimes corresponds to about  $\Phi = 0.886$ , where the relative hydration remains practically temperature independent. Interestingly this boundary remains roughly the same for PEO of different chain lengths. The explanation why the transition occurs at that particular polymer volume fraction is not readily evident, apart from the fact that approximately at this concentration hydrogens of hydroxyl groups start to lose water and associate with PEO according to Figure 2. It seems that this concentration indicates the boundary between water-dominated end group association to PEO-dominated end group association.

On the basis of results presented in Figures 4–6, one can conclude that the contribution of hydration via end groups becomes especially important in the poor hydration conditions (high temperature, high polymer concentration). As a result the answer to the question of what is the critical chain length when end group contribution to hydration becomes negligible becomes dependent on the conditions. If one considers 1% relative hydration as a critical boundary then  $N_{cr}^h \approx 250$  for  $\Phi = 0.5$  at  $T = 20\text{ }^{\circ}\text{C}$  but it is  $N_{cr}^h \approx 460$  for  $\Phi = 0.9$  at  $T$

= 20 °C and it is  $N_{cr}^h \approx 290$  for  $\Phi = 0.5$  at  $T = 200$  °C. Therefore, in general, the influence of end groups can be of some importance for the PEO of up to 10 000–20 000 molecular weight, which will be supported by our predictions for the phase behavior discussed below.

**Gelation.** Taking into account extensive hydrogen bonds in water,<sup>26</sup> any polymer forming multiple hydrogen bonds with water automatically becomes a part of the network of hydrogen bonds. At the same time, taking into account physical properties of water, it is rarely considered to be a gel, and similarly, any polymer immersed in water (even if forming hydrogen bonds with water) is not necessarily considered to be a part of a gel. With respect to PEO, there is a long standing discussion whether it forms clusters in water or it does not.<sup>5,18–21</sup> It seems that the answer depends on method of sample preparation and measurement procedure. Those researchers who did observe some indication of cluster formation have noted the molecular weight, concentration, and temperature dependence.<sup>5,18,21</sup> It seems that there might be some type of physical cross-linking (by means of hydrogen bonds) between the polymer which is somewhat stronger than a traditional network of hydrogen bonds in water.<sup>26</sup> Here we attempt to take a closer look at this issue.

Evidently, the strongest physical cross-links between different molecules can be achieved by direct hydrogen bonding. However this possibility exists only for hydroxyl-terminated PEO, and even then, it would require a high density of end groups to achieve the necessary degree of cross-linking. Since there is a large degree of hydrogen bonding between polymer and water, it is hard to avoid water involvement in formation of possible PEO clusters. On the other hand connection of different PEO molecules through the network of water–water hydrogen bonds cannot be strong as we discussed above. Therefore, the most “direct” physical cross-link between PEO molecules would be through a single water molecule, i.e., by two water–PEO hydrogen bonds. In such a case, the cross-link would be reasonably strong (consisting of two consecutive hydrogen bonds of  $\Delta E_{wp}/k = 2000$  K each) and the fraction of such cross-links would depend on polymer length, concentration, and temperature. Naturally direct PEO–PEO hydrogen bonding should also be allowed to contribute the cross-linking, as well as PEO–water hydrogen bonding as a part of single water molecule bridge. Applying classical gelation theory<sup>31–33</sup> for this case, we can write the following set of equations for the (extinction) probabilities  $v_i$  that formation of a hydrogen bond (by donating or accepting a proton) does not lead to infinite network formation

$$v_h = [1 + s_1(v_h - 1) + x(v_{wh} - 1)]^{2(N+m_0)} \times [1 + s(v_o - 1) + u(v_{wo} - 1)]^{m_h-1} \quad (20)$$

$$v_o = [1 + s_1(v_h - 1) + x(v_{wh} - 1)]^{2(N+m_0)-1} \times [1 + s(v_o - 1) + u(v_{wo} - 1)]^{m_h} \quad (21)$$

$$v_{wh} = [1 + u_1(v_h - 1)]^2 [1 + x_1(v_o - 1)] \quad (22)$$

$$v_{wo} = [1 + u_1(v_h - 1)][1 + x_1(v_o - 1)]^2 \quad (23)$$

where

$$\begin{aligned} x_1 &\equiv \frac{n_{wp}}{2N_w} = x \frac{\Phi v(N + m_0)}{(1 - \Phi)v_p(N + v_o)}; \\ u_1 &\equiv \frac{n_{pw}}{2N_w} = u \frac{m_h \Phi v}{2(1 - \Phi)v_p(N + v_o)}; \\ s_1 &\equiv \frac{n_{pp}}{2N_p(N + m_0)} = s \frac{m_h}{2(N + m_0)} \quad (24) \end{aligned}$$

are the probabilities to find a water–PEO hydrogen bond at a donor site of water,  $x_1$ , a PEO–water hydrogen bond at an acceptor site of water,  $u_1$ , and a PEO–PEO hydrogen bond at an acceptor site of PEO,  $s_1$ .  $v_h$  (or  $v_{wh}$ ) is the probability that a hydrogen bond formed by proton donation from the terminal hydroxyl groups of PEO (or from a water molecule) will lead to a finite-size chain. Similarly,  $v_o$  (or  $v_{wo}$ ) is the probability that a hydrogen bond formed at an acceptor site of PEO (or of a water molecule) will lead to a finite-size chain. Upon substitution of the latter two equations of the set into the former two  $v_{wo}$  and  $v_{wh}$  can be eliminated and our further discussion will concern only  $v_o$  and  $v_h$ . Below some critical degree of cross-linking the probability that a hydrogen bond formation leads to a finite size chain is one, i.e.,  $v_h = 1$  or  $v_o = 1$ , whereas above this point there is a gel formed by either direct PEO–PEO hydrogen bonds or through a single water-molecule cross-link (PEO–water–PEO) and  $v_h < 1$ ,  $v_o < 1$ . The critical point can be defined by considering a small deviation from the critical “conversion”

$$\epsilon = s - s_{cr}; \quad \epsilon = x - x_{cr}; \quad \epsilon = u - u_{cr} \quad (25)$$

and expanding  $v_h$ ,  $v_o$  in the power series of  $\epsilon$ :<sup>34</sup>

$$v_h = 1 + A_1\epsilon + A_2\epsilon^2 + \dots \quad (26)$$

$$v_o = 1 + B_1\epsilon + B_2\epsilon^2 + \dots \quad (27)$$

Substituting eqs 25–27 into eqs 20 and 21 and using eqs 22 and 23, we get the following equation for the gel point:

$$\begin{aligned} 1 - 2m_h s + m_h \left(1 + \frac{m_h - 1}{2(N + m_0)}\right) s^2 - \\ (2(N + m_0) - 1) \frac{\Phi v(N + m_0)}{(1 - \Phi)v_p(N + v_o)} x^2 + \\ \frac{m_h(1 - m_h)\Phi v}{2(1 - \Phi)v_p(N + v_o)} u^2 - \frac{4m_h\Phi v(N + m_0)}{(1 - \Phi)v_p(N + v_o)} xu + \\ 2 \frac{(2(N + m_0) - 1 + m_h)m_h\Phi v}{(1 - \Phi)v_p(N + v_o)} sxu + \\ \frac{3(N + m_0)(2(N + m_0) - 1 + m_h)(\Phi v)^2}{((1 - \Phi)v_p(N + v_o))^2} x^2 u^2 = 0 \quad (28) \end{aligned}$$

We note that in the case of methyl-terminated PEO, there is only one mechanism of cross-linking via a single water molecule by mean of water–PEO hydrogen bonds. In other words in this case  $s = 0$  and  $u = 0$  and the eq 28 becomes



$$\frac{1}{2(N + m_0) - 1} = \frac{\Phi v(N + m_0)}{(1 - \Phi)v_p(N + v_0)} x^2 \equiv xx_1 \quad (29)$$

The physical meaning of this equation becomes straightforward if we note that the number of water molecules connected to PEO (via water–PEO hydrogen bonds) by both hydrogens is  $n_{\text{cross}} = x_1^2 \mathcal{N}_w$ . These water molecules act as an active cross-links for the PEO molecules. The ratio of such cross-links to the total number of PEO molecules in the system characterizes the degree of cross-linking and using eq 29 this ratio is

$$\frac{n_{\text{cross}}}{\mathcal{N}_p} = \frac{x_1^2 \mathcal{N}_w}{\mathcal{N}_p} = x_1 x (N + m_0) = \frac{1}{2 - 1/(N + m_0)} \quad (30)$$

In the limit of long PEO chains  $N \rightarrow \infty$ , the ratio  $n_{\text{cross}}/\mathcal{N}_p \rightarrow +1/2$ , which has a straightforward meaning: to form a gel it is required to have more than one cross-link per two chains. Of course, the cross-link will be effective only if a water molecule is connecting different PEO chains, rather than different monomers of the same chain. As we mentioned above our model is not designed for description of intramolecular ring formation, so it is valid only above the overlap chain concentration where the probability to form intra- and intermolecular bonds is the same. As is expected from eq 30, the sol–gel transition should strongly depend on chain length. Figure 7 shows the sol–gel transition for methyl-terminated PEO chains of two different molecular weights ( $N = 5$  and  $N = 100$ ). As one can see with an increase of chain length the area of possible gel formation increases dramatically, expanding to larger concentration and temperature range.

For PEO chains terminated with at least one hydroxyl groups, two more types of hydrogen bonds (PEO–PEO and PEO–water) can participate in the physical cross-linking. As a result the area of possible gel formation expands in this case as well. As we discussed above, the influence of end groups is especially noticeable for short PEO chains, so we compare in Figure 7 the possible gel area for methyl and one methyl one hydroxyl-terminated PEO for  $N = 5$ . As one can see, replacement of one methyl group on hydroxyl group has a dramatic difference: the gel area increases until the size approximately corresponding to the methyl-terminated PEO chain of length  $N = 10$  (not shown). For both-end hydroxyl-terminated PEO having  $N = 5$ , the increase in the gel area (compared to the methyl-terminated chain) is even more striking. Now a gel can also be formed at a very high temperature and high polymer concentration. For one- or both-end methyl-terminated PEO in the area of high polymer concentration, gel formation is hardly possible due to the lack of cross-linking water. For hydroxyl-terminated PEO, the gel can be formed in this area by direct PEO–PEO hydrogen bonds. If one neglects any indirect (i.e., through water) cross-links, then only the first three terms in eq 28 would survive and the critical conversion would be

$$s_{\text{cr}} = \frac{1 - \sqrt{1 - \frac{1}{m_h} \left( 1 + \frac{m_h - 1}{2(N + m_0)} \right)}}{1 + \frac{m_h - 1}{2(N + m_0)}} \quad (31)$$

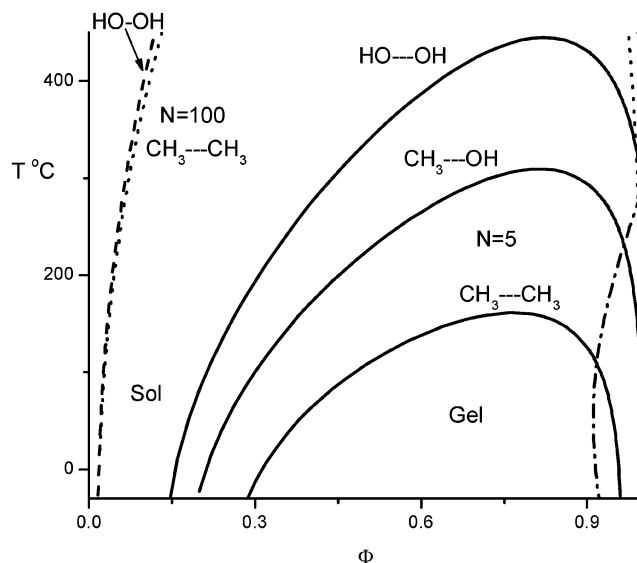


**Figure 7.** Sol–gel transition for the network formed by direct PEO–PEO hydrogen bonds and by single water-mediated PEO–H<sub>2</sub>O–PEO hydrogen bonds for  $N = 5$  (solid curves) and  $N = 100$  (dashed curve and dotted curve). The type of end group is indicated near the curves. The curves are obtained using eq 28 for  $\Delta E_{\text{wp}}/k = 2000$  K,  $\Delta E_{\text{ww}}/k = 1800$  K,  $\Delta E_{\text{pp}}/k = 1800$  K,  $\Delta E_{\text{pw}}/k = 2200$  K,  $\Delta_{\text{wp}} = \pi/8.35$ ,  $\Delta_{\text{ww}} = \pi/4.75$ ,  $\Delta_{\text{pp}} = \pi/10$ , and  $\Delta_{\text{pw}} = \pi/5$ . The area for the gel formed by direct PEO–PEO hydrogen bonds (eq 31) for hydroxyl-terminated PEO of  $N = 5$  is shown as dash-dot curve.

We note that in the case of PEO terminated by one hydroxyl group (and one methyl group)  $s_{\text{cr}} = 1$ . For the case of infinitely long PEO chains with both-end hydroxyl groups we get  $s_{\text{cr}}|_{N \rightarrow \infty} = 1 - 1/\sqrt{2}$ . The boundary for the gel formed only by direct PEO–PEO hydrogen bonds is also shown (as a dash-dot curve) in Figure 7. The width of this region varies with temperature, having a maximum at about  $T = 50$  °C. In general, the shorter the PEO chain the larger the PEO–PEO gel region, but it is much smaller than the overall gel area obtained considering both direct (PEO–PEO) and indirect (through a single water molecule) hydrogen bonding cross-links. For longer PEO chains the influence of end group (and direct PEO–PEO mechanism of cross-links) is minimal and even for  $N = 100$  the boundary of the possible gel region is almost the same for methyl- and hydroxyl-terminated PEO.

On the basis of the above calculations the possibility of cluster (gel) formation by means of the hydrogen bonds in PEO aqueous solutions cannot be excluded. However the question remains is whether these cross-links (hydrogen bonds) are strong enough to be noticed by the usual experimental techniques. There might also be a contribution from simple chain entanglements, but the latter must be of little concern for relatively dilute solutions or short PEO chains. Obviously the effect of entanglement should be the same for PEO with different terminal groups. So if, by changing terminal groups from methyl to hydroxyl, one observes enhancement of cluster formation for short PEO chains, then it must be due to hydrogen bonding cross-links. We note that besides entanglement there are other factors which may influence gel formation.<sup>24,35–38</sup> For instance, due to the change of chain conformation (e.g., with temperature), part of the hydrogen bonds may become inaccessible for cross-linking<sup>35,37</sup> or ring formation can contribute to the gel formation.<sup>24,36,38</sup> To consider these factors in neces-

sary detail, the whole approach should be generalized to account for the atomistic structure of the polymer and solute.

**Second Virial Coefficient.** As we discussed in our previous paper,<sup>7</sup> hydrogen bonding between PEO and water is the reason for PEO solubility and its decrease with increasing temperature. To calculate the second virial coefficient, one can consider the expansion of the osmotic pressure into the power series of the volume fraction of polymer around zero polymer concentration:

$$\Pi = \Pi_0 + \left( \frac{\partial \Pi}{\partial \Phi} \right) \Big|_{\Phi=0} \Phi + \frac{1}{2} \left( \frac{\partial^2 \Pi}{\partial \Phi^2} \right) \Big|_{\Phi=0} \Phi^2 + \dots \quad (32)$$

The coefficient of the quadratic term gives us the value of the second virial coefficient:

$$A_2 = \frac{1}{2} \left( \frac{\partial^2 \Pi}{\partial \Phi^2} \right) \Big|_{\Phi=0} \quad (33)$$

After the corresponding (straightforward but somewhat cumbersome) calculations we get for the second virial coefficient  $A_2$ :

$$A_2 = \frac{1}{2} - \chi + \frac{2}{1 + y_0} \times \left( x_0 \frac{(N + m_0)v}{(N + v_e)v_p} - y_0 + \frac{1}{2} \frac{x_0^2}{(1 - y_0)} \left( \frac{(N + m_0)v}{(N + v_e)v_p} \right)^2 \right) + \frac{2}{1 + y_0} \left( u_0 \frac{m_h v}{2(N + v_e)v_p} + \frac{1}{2} \frac{u_0^2}{(1 - y_0)} \left( \frac{m_h v}{2(N + v_e)v_p} \right)^2 \right) - \frac{m_h(N + m_0)v^2}{(N + v_e)^2 v_p^2} \left[ \frac{x_0 y_0 u_0}{1 - y_0^2} + 2 \exp \left( \frac{\Delta E_{pp}}{kT} - \Delta S_{pp} \right) \times (1 - u_0)(1 - x_0) \right] \quad (34)$$

where  $x_0$ ,  $y_0$ , and  $u_0$  are the corresponding degrees of association in the zero polymer concentration limit. As expected, eq 34 assumes the form of eq 28 from our previous paper<sup>7</sup> in the limit of long chains, when end effects becomes negligible. As before, the signs of different terms in eq 34 indicate that interspecies hydrogen bonding (such as water–PEO ( $x_0$ ) or PEO–water ( $u_0$ )) leads to an increase in the second virial coefficient and improves solubility of the polymer, whereas intraspecies hydrogen bonding (such as water–water ( $y_0$ ) or PEO–PEO) decreases the  $A_2$  and the polymer solubility. As we discussed above, with the temperature increase the interspecies hydrogen bonding decreases at much quicker rate than for intraspecies that leads to the decrease of polymer solubility and results in phase separation at high temperatures. The temperature dependence of the second virial coefficient closely follows the behavior discussed in our previous paper for long chains (neglecting end effects).<sup>7</sup> Therefore, here we will discuss mainly the chain length dependence of the second virial coefficient.

The chain length dependence of the second virial coefficient at  $T = 20^\circ\text{C}$  is shown in Figure 8 for the PEO chains terminated by different end groups. For hydroxyl-terminated PEO (at one or both ends) the second virial coefficient decreases with an increase in

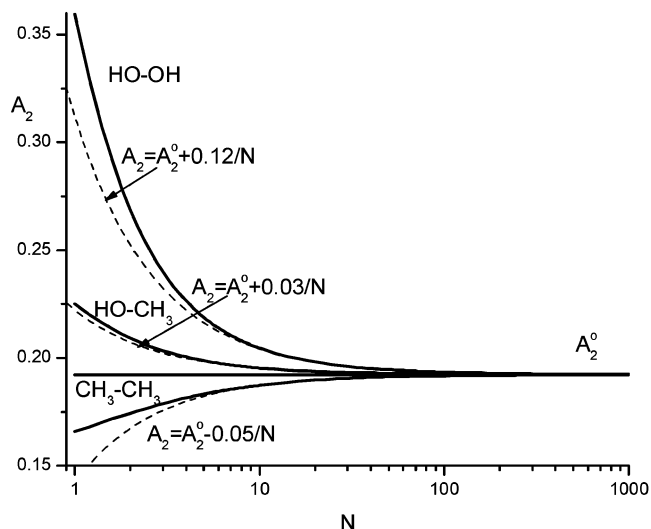


**Figure 8.** Second virial coefficient for aqueous solutions of PEO as a function of polymer chain length for both-end hydroxyl-terminated (HO–OH), one-end hydroxyl and one methyl-terminated (HO–CH<sub>3</sub>) and both end methyl-terminated PEO (CH<sub>3</sub>–CH<sub>3</sub>). Approximation by the scaling laws are shown by dashed lines. The curves are obtained using eq 34 for  $T = 20^\circ\text{C}$ ,  $\Delta E_{wp}/k = 2000\text{ K}$ ,  $\Delta E_{ww}/k = 1800\text{ K}$ ,  $\Delta E_{pp}/k = 1800\text{ K}$ ,  $\Delta E_{pw}/k = 2200\text{ K}$ ,  $\Delta_{wp} = \pi/8.35$ ,  $\Delta_{ww} = \pi/4.75$ ,  $\Delta_{pp} = \pi/10$ ,  $\Delta_{pw} = \pi/5$ , and  $\chi = -0.209 + 93.5/T$ .

PEO chain length. For both-ends hydroxyl-terminated PEO  $A_2$  follows the  $A_2 = A_2^0 + 0.12/N$  scaling law, tending to a constant level for long PEO chains ( $A_2|_{N \rightarrow \infty} = A_2^0$ ). For the PEO chains terminated by one methyl and one hydroxyl groups,  $A_2$  also decreases with  $N$ , although the influence of one hydroxyl group is considerably weaker:  $A_2 = A_2^0 + 0.03/N$ . Experimental data confirm the tendency for a slight decrease in the second virial coefficient for hydroxyl-terminated PEO.<sup>5,6,19,39</sup> Most of results were obtained for relatively long PEO where the trend is rather weak.<sup>5,6,19,39</sup> One report for somewhat lower molecular weight PEO confirms a stronger decrease in  $A_2$  with  $N$ ,<sup>40</sup> however due to experimental uncertainties a direct comparison of experimental data with theoretical predictions remains rather difficult. We expect the most dramatic effect of end groups to be observed for the short PEO (PEG) chains,  $N \leq 20$ . For PEO chains terminated by methyl groups at both ends the second virial coefficient slightly increases with an increase in PEO chain length. This increase can be approximated as  $A_2 = A_2^0 - 0.05/N$ . This difference in the behavior of the second virial coefficient is due to interactions between the end groups and water. For hydroxyl groups there are additional hydrogen bonds formed between PEO and water by proton donation from end groups, and therefore, there are more interspecies hydrogen bonds leading to an increase in  $A_2$ . For methyl groups there is no additional hydrogen bonding between the end groups and water and in addition the end groups occupy more volume. Therefore, for methyl-terminated PEO there are fewer interspecies hydrogen bonds per unit volume of the polymer (compared to hydroxyl-terminated PEO), and the second virial coefficient is smaller in this case. In all cases, the effect of end groups becomes noticeable only for relatively short chains, and its contribution decreases as  $1/N$  similar to the relative hydration.

**Phase Diagram.** To calculate the phase diagram we can first define the regions of absolute instability of the

homogeneous phase by analyzing the second derivative of the free energy (eq 8) with respect to  $\Phi$ . The regions where  $d^2F/d\Phi^2 \leq 0$  are the instability regions. Hence to find the spinodal of macrophase separation we need to calculate  $d^2F/d\Phi^2 = 0$ . The result of such calculations is

$$\begin{aligned} & \frac{(1-m_h)v}{\Phi(N+v_e)v_p} - \frac{1}{1-\Phi} - 2\chi + 2 \frac{\left(1-y+x \frac{(N+m_o)v}{(N+v_e)v_p}\right)^2}{(1-\Phi)Z} \times \\ & \left(1 - s^2 \frac{m_h}{2(N+m_o)} - u^2 \frac{\Phi m_h v}{2(1-\Phi)(N+v_e)v_p}\right) + \\ & \frac{m_h v(-1+s-u\Phi/(1-\Phi))^2}{\Phi(N+v_e)v_p Z} \times \\ & \left(1 - y^2 - x^2 \frac{\Phi}{(1-\Phi)} \frac{(N+m_o)v}{(N+v_e)v_p}\right) + \\ & \frac{2m_h v(-1+s-u\Phi/(1-\Phi))}{(1-\Phi)(N+v_e)v_p Z} \left(1 - y + x \frac{(N+m_o)v}{(N+v_e)v_p}\right) \times \\ & (yu + xs) = 0 \quad (35) \end{aligned}$$

where

$$\begin{aligned} Z = & \left(1 - y^2 - x^2 \frac{\Phi}{(1-\Phi)} \frac{(N+m_o)v}{(N+v_e)v_p}\right) \times \\ & \left(1 - s^2 \frac{m_h}{2(N+m_o)} - u^2 \frac{\Phi m_h v}{2(1-\Phi)(N+v_e)v_p}\right) - \\ & \frac{\Phi m_h v}{2(1-\Phi)(N+v_e)v_p} (yu + xs)^2 \end{aligned}$$

It is easy to see that in the limit when there is no hydrogen bonding ( $x \rightarrow 0$ ,  $y \rightarrow 0$ ,  $s \rightarrow 0$ ,  $u \rightarrow 0$ ) eq 35 assumes the usual Flory–Huggins form for the spinodal of nonassociated polymer solution:  $v/(N\Phi v_p) + 1/(1-\Phi) - 2\chi = 0$ . Moreover, in the limit when there is no hydrogen bonding via terminal groups, i.e., when  $s \rightarrow 0$ ,  $u \rightarrow 0$ , eq 35 coincides with eq 31 derived in our previous paper, where end effects have been neglected.<sup>7</sup>

Differentiating the free energy (eq 8) with respect to polymer volume fraction and using the equations for the average degree of the different associations (eqs 12–15), we obtain the (reduced) chemical potential ( $\mu = dF/d\Phi$ ) and osmotic pressure ( $\Pi = \mu\Phi - F$ )

$$\begin{aligned} \frac{\mu}{kT} = & \frac{v}{(N+v_e)v_p} \ln \frac{\Phi v}{(N+v_e)v_p} - \ln(1-\Phi) + \\ & \chi(1-2\Phi) + 2 \frac{(N+m_o)v}{(N+v_e)v_p} \ln \left(1 - x - s \frac{m_h}{2(N+m_o)}\right) + \\ & \frac{m_h v}{(N+v_e)v_p} \ln(1-u-s) - \\ & 2 \ln \left(1 - y - x \frac{\Phi(N+m_o)v}{(1-\Phi)(N+v_e)v_p}\right) - \\ & 2 \ln \left(1 - y - u \frac{\Phi m_h v}{2(1-\Phi)(N+v_e)v_p}\right) \quad (36) \end{aligned}$$

$$\frac{\Pi}{kT} = \frac{\Phi v}{(N+v_e)v_p} - \ln(1-\Phi) + 1 - \Phi - \chi\Phi^2 -$$

$$\begin{aligned} & 2\Phi \frac{(N+m_o)v}{(N+v_e)v_p} x - \frac{\Phi m_h v}{(N+v_e)v_p} (u+s) - \\ & 2 \ln \left(1 - y - x \frac{\Phi(N+m_o)v}{(1-\Phi)(N+v_e)v_p}\right) - 2\gamma(1-\Phi) - \\ & 2 \ln \left(1 - y - u \frac{\Phi m_h v}{2(1-\Phi)(N+v_e)v_p}\right) \quad (37) \end{aligned}$$

To calculate the two phase equilibrium region one can use the set of equations for the chemical potential and pressure:

$$\begin{cases} \mu(\Phi_1) = \mu(\Phi_2) \\ \Pi(\Phi_1) = \Pi(\Phi_2) \end{cases} \quad (38)$$

By solving numerically the set of equations, one can obtain the volume fractions of polymer in each of the coexisting phases,  $\Phi_1$  and  $\Phi_2$  for a fixed temperature. By varying the temperature, the whole space of the phase diagram can be covered.

The phase diagram for aqueous solutions of PEO with different terminal groups is shown in Figure 9 in comparison with experimental data.<sup>1,3,4</sup> Compared to the previous results for long chains (neglecting end effects),<sup>7</sup> the overall appearance of the phase diagram is somewhat similar. However, there are several important nuances. One of the main differences is in the better agreement for shorter chains  $N \lesssim 100$  between experimentally reported data and the theoretical predictions of the present model. For instance, experimental data for  $M_w = 3350$  ( $N \approx 76$ )<sup>4</sup> closely match the theoretical curve for  $N = 76$  (in the previous model,<sup>7</sup> it was approximated by the curve with  $N = 55$ ), and the data for  $M_w = 2180$  ( $N \approx 50$ )<sup>3</sup> and  $M_w = 3000$  ( $N \approx 68$ )<sup>1</sup> even though being inconsistent with each other are closely distributed around the curve for  $N = 58$  (previously  $N = 39$ ), which is about the average between the two molecular weights. We also note that in the present model the theoretical curves are better centered around the experimental data, which is most noticeable for shorter chains. We note that here we used the same set of parameters as in our previous diagram,<sup>7</sup> except for slight adjustment of the  $\chi_o$ -parameter for PEO–water interactions without hydrogen bonding,  $\chi_o = -0.209 + 93.5/T$  (previously,  $\chi_o = -0.211 + 93.5/T$ ). The necessity of such an adjustment is connected with the strong influence of the end groups on the solubility of PEO. Even through the relative hydration of PEO changes with PEO chain length according to a  $1/N$  law, such a small increase as 1% in the interspecies degree of hydrogen bonding becomes noticeable close to the phase separation boundaries, defined by a delicate balance between repulsive volume interactions, translational entropy, and hydrogen bonding.

The effect of the end groups on the solubility of PEO chains in water is especially evident from analyzing their influence on the critical solution temperatures for aqueous solutions of PEO. The upper and lower critical solution temperatures (LCST and UCST) correspond to the extrema of the spinodal, eq 35. The predictions of our model for UCST (upper) and LCST (lower critical solution point) for PEO with different terminal groups



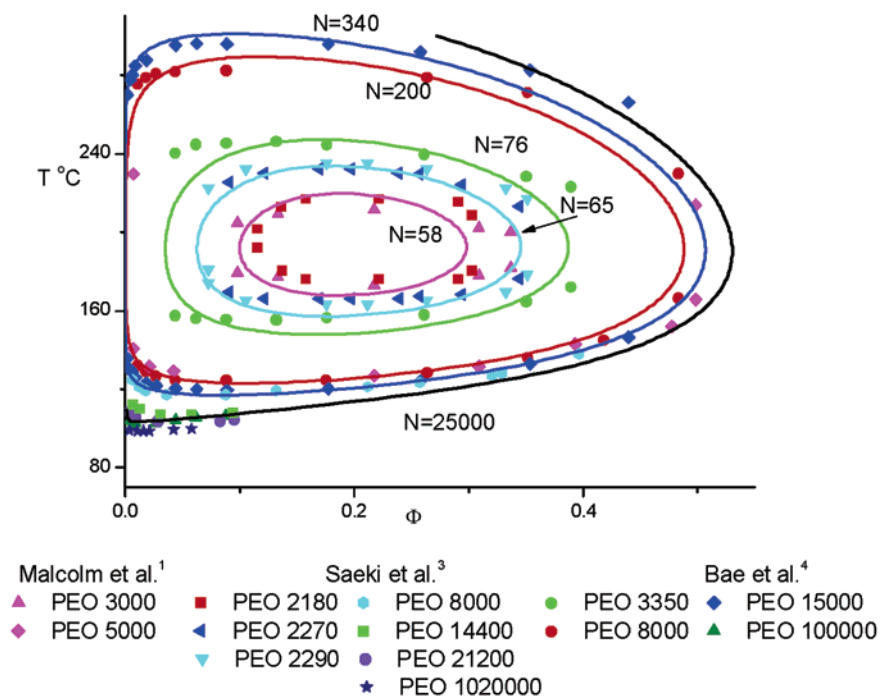


**Figure 9.** Phase diagram for aqueous solutions of hydroxyl-terminated PEO accounting for the end-effect. Experimental data<sup>1,3,4</sup> are represented by symbols. Theoretical curves are all calculated using the same set of parameters:  $\Delta E_{wp}/k = 2000$  K,  $\Delta E_{ww}/k = 1800$  K,  $\Delta E_{pp}/k = 1800$  K,  $\Delta E_{pw}/k = 2200$  K,  $\Delta_{wp} = \pi/8.35$ ,  $\Delta_{ww} = \pi/4.75$ ,  $\Delta_{pp} = \pi/10$ ,  $\Delta_{pw} = \pi/5$ , and  $\chi = -0.209 + 93.5/T$ . The PEO polymerization number employed for calculating each of the curves is shown near the curves.

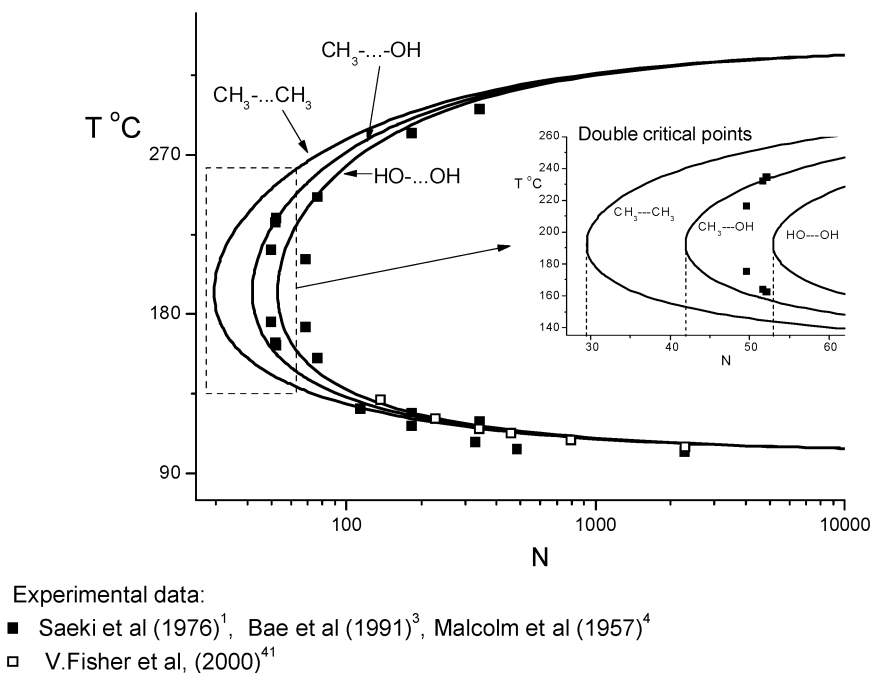


**Figure 10.** Critical solution temperatures for aqueous solutions of PEO with different terminal groups as a function of PEO chain length. Experimental data<sup>1,3,4,41</sup> are shown as different symbols. The area close to the double critical points is shown in magnification in the insert. Theoretical curves are calculated using the same set of parameters as for the phase diagram in Figure 9:  $\Delta E_{wp}/k = 2000$  K,  $\Delta E_{ww}/k = 1800$  K,  $\Delta E_{pp}/k = 1800$  K,  $\Delta E_{pw}/k = 2200$  K,  $\Delta_{wp} = \pi/8.35$ ,  $\Delta_{ww} = \pi/4.75$ ,  $\Delta_{pp} = \pi/10$ ,  $\Delta_{pw} = \pi/5$ , and  $\chi = -0.209 + 93.5/T$ .

are shown in Figure 10 in comparison with experimental data.<sup>1,3,4,41</sup> As expected, the experimental data for LCST and UCST corresponding to the data in the phase diagram (Figure 9)<sup>1,3,4</sup> closely match the theoretical predictions for PEO terminated from both ends by hydroxyl groups. Moreover, when we added to the plot the recent experimental data for the LCST and UCST obtained by Fisher et al.,<sup>41</sup> they precisely match the

theoretical curve. Comparing the critical points (UCST and LCST) for polymer chains terminated by different end groups, it becomes evident that while all curves merge in the long chain limit, they considerably deviate from each other at shorter chains lengths. For the LCST the curves for different end groups merge at  $N \approx 300$ , whereas for UCST it happens at higher  $N$ ,  $N \approx 500$ . This result is not surprising taking into account that,

as we discussed above, hydroxyl end groups remain hydrogen bonded with water in the poor hydration region, e.g., at high temperatures, therefore increasing the contribution of end groups to polymer solubility at the UCST to a larger extent than at the LCST.

At shorter chain length, the UCST and LCST (and similarly  $\min(\Phi_1)$  and  $\max(\Phi_2)$  corresponding to the polymer concentrations in coexisting phases at the maximal width of phase separation area) start to approach each other, merging at the so-called double critical point ( $T_{cr}$ ,  $N_{cr}$ ).<sup>42,43</sup> At chain lengths less than  $N_{cr}$  (corresponding to the double critical point) the aqueous solutions of PEO are stable over the whole concentration and temperature range. For PEO above this critical molecular weight, there will be a closed-loop region of phase coexistence for some temperature and concentration range. The larger the molecular weight, the wider the temperature and concentration range of phase coexistence will be. The characteristic feature of the double critical point is that critical exponents of the different thermodynamic quantities (which are not temperature derivatives of the thermodynamic potential of the Landau model), such as correlation length exponent,  $\nu$  ( $\xi \sim |T - T_{cr}|^{-\nu}$ ), the susceptibility/compressibility exponent,  $\gamma$ , viscosity, etc., are doubled at the double critical point compared to their normal value, i.e., replaced by  $2\nu$ ,  $2\gamma$ , etc.<sup>42–44</sup> For hydroxyl-terminated PEO chains, the double critical point corresponds to  $N_{cr} = 53$ , for one end hydroxyl, one end methyl group terminated PEO it is reached at  $N_{cr} = 42$ , and for methyl-terminated chains it is  $N_{cr} = 30$  (Figure 10). For all three cases, the critical temperature is practically the same,  $T_{cr} \approx 192$  °C. The considerable difference in  $N_{cr}$  for PEO chains with different terminal groups confirms the strong influence of the hydration via hydroxyl end groups on solubility of PEO. The practical implication of this result is that termination of a relatively short PEO chain by hydroxyl groups may substantially improve its solubility in water compared to methyl-terminated chain. This conclusion is consistent with observations by Medved' et al.<sup>15</sup> that termination of PEO by more hydrophobic end groups considerably decreases its LCST and solubility. On the basis of the results presented in Figure 10, termination of PEO by one hydroxyl group improves the solubility of PEO chains to an extent that it is equivalent to decreasing of chain length of methyl-terminated PEO by about 10 monomer units; adding another hydroxyl group doubles the effect. The effect of the end groups on phase behavior of PEO remain noticeable for PEO chain up to 250–500 repeat units long.

## Conclusions

In the present paper we have used a statistical mean-field model to analyze the influence of terminal end groups on the phase behavior and properties of PEO. We have considered the typical end groups industrially used for PEO termination: both ends terminated by methyl groups, one end methyl and one end hydroxyl groups, and both ends hydroxyl groups. We found that, in general, methyl-terminated PEO behaves in a similar way as long PEO, i.e., the influence of end groups is almost negligible. Hydroxyl-terminated PEO (from one and especially both ends) behaves quite differently, especially for a relatively short chain lengths. We have generalized our previous model to account for the competition for proton donors and acceptors among four

types of hydrogen bonding (donors are mentioned first): water–PEO, water–water, PEO–water, and PEO–PEO. PEO–PEO hydrogen bonding is the weakest among the four, and it becomes noticeable only at high polymer concentration region (Figure 2). PEO–water hydrogen bonding (via hydroxyl group proton donation) is the strongest and the corresponding degree of association is close to one in a wide range of concentration and temperature (Figures 2 and 3). It decreases only at high polymer concentration region due to competition with PEO–PEO hydrogen bond formation and at high temperatures when any type of hydrogen bonding becomes less favorable (compared to  $kT$ ).

The general effect of end groups is 2-fold: it increases the overall hydration and enhances the possibility of physical cross-linking among different PEO molecules. Polymer hydration can be characterized via the hydration number (the number of hydrogen bonded water molecules per repeat unit of PEO), which decreases with an increase in temperature and polymer concentration (Figure 4). The contribution of end groups to the overall hydration becomes noticeable especially for the short chains. To estimate the influence of end group hydration we considered the relative hydration, i.e., the ratio of the number of water molecules hydrogen bonded to end groups compared to those hydrogen bonded to PEO repeat units. We found that for short chains ( $N \leq 10$ ) the hydration via end groups is comparable with hydration of the main chain (Figure 5). For longer PEO chains the contribution of end groups to the overall hydration decreases following a  $1/N$  law, but it remains larger than 1% for chains with fewer than 250 ( $\Phi = 0.5$ ) or even 460 ( $\Phi = 0.9$ ) monomer units. Comparing different polymer concentrations and temperatures, we found that the *contribution of the end group to the hydration becomes especially important in the poor hydration regions, i.e., at high polymer concentration (low water content) and at high temperature* (Figure 6).

Physical cross-linking of PEO can occur either by direct PEO–PEO hydrogen bonding or via water molecule bridges. For methyl-terminated PEO, the only possible mechanism of PEO cross-linking is via water. It is reasonable to expect that cross-linking via a single water molecule hydrogen bonded with different PEO chains is stronger than through the network of water–water hydrogen bonding. Accounting only for the former we found that the sol–gel transition can occur only when there are more than one cross-linking water molecules per two molecules of PEO:  $n_{\text{cross}}/N_p = 1/[2 - 1/(N + m_0)]$ . The corresponding gel area strongly increases with chain length  $N$ . For hydroxyl-terminated PEO there is also direct PEO–PEO cross-linking, which is noticeable only at high polymer concentration and PEO–water–PEO cross-linking though proton donation of hydroxyl groups. Because of these additional mechanisms of cross-linking the possible gel area considerably expands into a larger concentration and temperature range (Figure 7). There still remains a question whether such physical cross-linking is strong enough (e.g., compared to simple entanglement) to be of experimental importance and could explain cluster formation which has been reported by a few workers.<sup>5,18,21</sup> However, it would definitely be the case that hydroxyl-terminated short chain PEO would have a larger degree of cross-linking compared to the methyl-terminated one.

End groups have also impact on the behavior of the second virial coefficient,  $A_2$ . As we discussed in our previous paper, interspecies hydrogen bonding enhances solubility of the polymer and leads to an increase of  $A_2$ , whereas intraspecies hydrogen bonding has the opposite effect. For PEO terminated by one or two hydroxyl groups (Figure 8), the second virial coefficient decreases with an increasing chain length as  $A_2 = A_2^0 + 0.03/N$ , or  $A_2 = A_2^0 + 0.12/N$ , respectively (where  $A_2^0$  is the second virial coefficient in the limit of infinitely long chain ( $A_{2|N \rightarrow \infty} = A_2^0$ ). This effect is easy to understand since each hydroxyl group brings additional interspecies hydrogen bonding (PEO–water) that enhances the solubility of PEO and is the most noticeable for short chains. Experimental data<sup>19,39,40</sup> confirm the tendency for a slight decrease in the second virial coefficient for hydroxyl-terminated PEO, although most of the results were obtained for relatively long PEO<sup>19,39</sup> where the trend is relatively weak. For methyl-terminated PEO, there is the opposite tendency, as the second virial coefficient slightly increases with  $N$ :  $A_2 = A_2^0 - 0.05/N$ . Methyl groups do not provide any additional hydrogen bonding but rather increase the volume occupied by chain and thus decreases the solubility and  $A_2$ .

We have also calculated the phase diagram for PEO in water taking into account end-effects (Figure 9). We found that the presence of hydroxyl end groups improves the solubility of polymers of small to moderate chain length  $N \lesssim 500$ , which is consistent with influence of end groups on relative hydration. The effect of hydroxyl end groups for the short chains  $N \lesssim 80$  is especially dramatic. For instance, experimental data for  $M_w = 3350$  ( $N \approx 76$ )<sup>4</sup> are closely distributed around the theoretical curve for  $N = 76$  (whereas in the previous model<sup>7</sup> it was approximated by the curve with  $N = 55$ ). We also note that in the present model the theoretical curves are better centered compared to experimental data, which is most noticeable for shorter chains. In general we found that accounting for the end-effect produces a phase diagram which closely matches experimental data<sup>1,3,4</sup> and is consistent in a larger range of molecular weights compared to the diagram obtained neglecting end effects.<sup>7</sup> This is especially evident when the predictions of our model for the UCST (upper-) and LCST (low critical solution point) are compared with the experimental results<sup>1,3,4,41</sup> (Figure 10). All data are situated close to the theoretical curve for aqueous solutions of hydroxyl-terminated PEO including recent experimental data by Fisher et al.<sup>41</sup> which precisely match our theoretical prediction. Comparing the critical points (UCST and LCST) for polymer chains terminated by different end groups it becomes evident that while all curves merge in the long chain limit ( $N > 300$  for LCST and  $N > 500$  for UCST), for shorter chain lengths the curves deviate from each other considerably, reaching double critical points (where the UCST merges with the LCST) at different  $N$ . Thus, for both-end hydroxyl-terminated chains, the minimal chain length when the phase separation starts is  $N_{cr} = 53$ , for one end hydroxyl, one end methyl group terminated PEO  $N_{cr} = 42$  and for both-ends methyl-terminated chains  $N_{cr} = 30$ . These results are consistent with observations by Medved' et al.<sup>15</sup> that termination of PEO by more hydrophobic end groups considerably decreases its LCST and solubility. We conclude that termination of PEO by one hydroxyl group improves the solubility of PEO chains to an extent that it is equivalent to

decreasing of chain length of methyl-terminated PEO by about 10 monomer units, adding another hydroxyl group doubles the effect. In general the effect of the end groups on phase behavior of PEO remain noticeable for PEO chain up to 250–500 repeat units long.

**Acknowledgment.** This work in part was supported by the Biomimetic and Bioactive Polymers Program of Case Western Reserve University. I would like to thank Dr. D. Bedrov (University of Utah) for calling to my attention the work of Medved' et al.<sup>15</sup>

## References and Notes

- (1) Malcolm, G. N.; Rowlinson, J. S. *Trans. Faraday. Soc.* **1957**, *53*, 921.
- (2) Bailey, F. E.; Callard, R. W. *J. Appl. Polym. Sci.* **1959**, *1*, 56.
- (3) Saeki, S.; Kuwahara, N.; Nakata, M.; Kaneko, M. *Polymer* **1976**, *17*, 685.
- (4) Bae, Y. C.; Lambert, S. M.; Soane, D. S.; Prausnitz, J. M. *Macromolecules* **1991**, *24*, 4403.
- (5) Strazielle, C. *Makromol. Chem.* **1968**, *119*, 50.
- (6) Venohr, H.; Fraaije, V.; Strunk, H.; Borchard, W. *Eur. Polym. J.* **1998**, *34*, 732.
- (7) Dormidontova, E. E. *Macromolecules* **2002**, *35*, 987.
- (8) Matsuyama, A.; Tanaka, F. *Phys. Rev. Lett.* **1990**, *65*, 341.
- (9) Bae, Y. C.; Shim, J. J.; Soane, D. S.; Prausnitz, J. M. *J. Appl. Polym. Sci.* **1993**, *47*, 1193.
- (10) Bekiranov, S.; Bruinsma, R.; Pincus, P. *Phys. Rev. E* **1997**, *55*, 577.
- (11) Smith, G. D.; Bedrov, D.; Borodin, O. *Phys. Rev. Lett.* **2000**, *85*, 5583.
- (12) Lacombe, R. H.; Sanchez, I. C. *J. Phys. Chem.* **1976**, *80*, 2568.
- (13) Chhajjar, M.; Gujrati P. D. *J. Chem. Phys.* **1998**, *109*, 9022.
- (14) Ruokolainen, J.; Mäkinen, R.; Torkkeli, M.; Mäkelä, T.; Serimaa, R.; ten Brinke, G.; Ikkala, O. *Science* **1998**, *280*, 557.
- (15) Ruzette, A. V. G.; Banerjee, P.; Mayes, A. M.; Pollard, M.; Russell, T. P.; Jerome, R.; Slawacki, T.; Hjeltn, R.; Thiagarajan, P. *Macromolecules* **1998**, *31*, 8509.
- (16) Cho, J. H. *Macromolecules* **2000**, *33*, 2228.
- (17) Allen, C.; Maysinger, D.; Eisenberg, A. *Colloids Surf. B* **1999**, *16*, 3.
- (18) Kwon, G. S.; Okano, T. *Adv. Drug Delivery Rev.* **1996**, *21*, 107.
- (19) Lee, J. H.; Lee, H. B.; Andrade, J. D. *Prog. Polym. Sci.* **1995**, *20*, 1043.
- (20) Medved', Z. N.; Bulgakova, M. B. *Zh. Prikl. Khim.*, **1980**, *53*, 1669.
- (21) Spitzer, M.; Sabadini, E.; Loh, W. *J. Braz. Chem. Soc.* **2002**, *13*, 7.
- (22) Frielinghaus, H.; Pedersen, W. B.; Larsen, P. S.; Almdal, K.; Mortensen, K. *Macromolecules* **2001**, *34*, 1096.
- (23) Brown, W. *Macromolecules* **1984**, *17*, 66.
- (24) Devanand, K.; Selser, J. C. *Macromolecules* **1991**, *24*, 5943.
- (25) Kinugasa, S.; Nakahara, H.; Fudagawa, N.; Koga, Y. *Macromolecules* **1994**, *27*, 6889.
- (26) Ho, D. L.; Hammouda, B.; Kline, S. R. *J. Polym. Sci., Part B: Polym. Phys.* **2003**, *41*, 135–138.
- (27) Hammouda, B.; Ho, D.; Kline, S. *Macromolecules* **2002**, *35*, 8578.
- (28) Semenov, A. N.; Rubinstein, M. *Macromolecules* **1998**, *31*, 1373.
- (29) We note that the free energy of the reference state as it introduced by Flory contains also the following (linear on  $\Phi$  or constant) terms:  $-(\Phi v(N-1)\ln[(z-1)/e])/(v_p(N+v_e)) + \Phi v/(v_p(N+v_e)) + 1 - \Phi$ , where  $z$  is the number of nearest neighbors in a lattice. Accounting for these terms would have the only effect of shifting the reduced chemical potential (eq 36) by the corresponding constant value:  $-(v(N-1)\ln[(z-1)/e])/(v_p(N+v_e)) + v/(v_p(N+v_e)) - 1$ . This constant shift cancels upon considering the phase equilibria between polymer-rich and solvent-rich phases (eq 38) and has no effect at all on any results discussed in this paper.
- (30) Erukhimovich, I.; Thamm, M. V.; Ermoshkin, A. V. *Macromolecules* **2001**, *34*, 5653.
- (31) Erukhimovich, I.; Ermoshkin, A. V. *J. Chem. Phys.* **2002**, *116*, 368.
- (32) Lüsse, S.; Arnold, K. *Macromolecules* **1996**, *29*, 4251.
- (33) Franks, F. *Water a Comprehensive Treatise*; Plenum: New York, 1973; Eisenberg, D.; Kauzmann, W. *The Structure and Properties of Water*; Clarendon: Oxford, England, 1969.
- (34) Prabhumirashi, L. S.; Jose, C. I. *J. Chem. Soc., Faraday Trans. 2* **1975**, *71*, 1545.
- (35) Lebedeva, T. L.; Igonin, V. E.;



- Feldstein, M. M.; Plate, N. A. *Proceed. Int. Symp. Controlled Release Bioactive Mater.* **1997**, 24, 447.
- (28) Bieze, T.W. N.; Barnes, A. C.; Huige, C. J. M.; Enderby, J. E.; Leyte, J. C. *J. Phys. Chem.* **1994**, 98, 6568.
- (29) Maisano, G.; Majolino, D.; Migliardo, P.; Venuto, S.; Aliotta, F.; Magazú, S. *Mol. Phys.* **1993**, 78, 42; Branca, C.; Magazú, S.; Maisano, G.; Migliardo, P.; Villari, V. *J. Phys.: Condens. Matter* **1998**, 10, 10141; Magazú, J. *Mol. Struct.* **2000**, 523, 47.
- (30) Sasahara, K.; Sakurai, M.; Nitta, K. *Colloid. Polym. Sci.* **1998**, 276, 643.
- (31) Flory, P. J. *J. Am. Chem. Soc.* **1941**, 63, 3083.
- (32) Stockmayer, W. H. *J. Chem. Phys.* **1964**, 41, 2389.
- (33) Dobson, G. R.; Gordon, M. *J. Chem. Phys.* **1965**, 42, 705; **1964**, 41, 2389.
- (34) Olemskoi, A. I.; Krakovsky, I. *Physica A*, **2001**, 291, 79.
- (35) Gujrati, P. D.; Bowman, D. D. *J. Chem. Phys.* **1999**, 111, 8151.
- (36) Gujrati, P. D. *J. Phys. A: Math. Gen.* **2001**, 34, 9211.
- (37) Tanaka, F. *Macromolecules* **2000**, 33, 4249.
- (38) Erukhimovich, I.; Ermoshkin, A. V. *JETP* **1999**, 88, 538.
- (39) Kawaguchi, S.; Imai, G.; Suzuki, J.; Miyahara, A.; Kitano, T.; Ito, K. *Polymer* **1997**, 38, 2885.
- (40) Wang, S.-C.; Wang, C.-K.; Chang, F.-M.; Tsao, H.-K. *Macromolecules* **2002**, 35, 9551.
- (41) Fisher, V.; Borchard, W. *J. Phys. Chem. B.* **2000**, 104, 4463.
- (42) Landau, L. D.; Lifshitz, E. M. *Statistical Physics, Part 1*, 3rd ed.; Pergamon: New York, 1980.
- (43) Walker, J. S.; Vause, C. A. *J. Chem. Phys.* **1983**, 79, 2660; Goldstein, R. E.; Walker, J. S. *J. Chem. Phys.* **1983**, 78, 1492; Walker, J. S.; Vause, C. A. *J. Sci. Am.* **1987**, 256, 98.
- (44) Johnston, R. G.; Clark, N. A.; Witzius, P.; Cannell, D. S. *Phys. Rev. Lett.* **1985**, 54, 49; Larsen, G. A.; Sorensen, C. M. *Phys. Rev. Lett.* **1985**, 54, 343.

MA035609+